# Microstructure and phase composition of an alloy of iron and chrome disilicides

© E.I. Suvorova[1], F.Yu. Solomkin[2], N.A. Arkharova[1], N.V. Sharenkova[2], G.N. Isachenko[2]

[1] Federal Research Center „Crystallography and Photonics"
Shubnikov Institute of Crystallography, Russian Academy of Sciences,
119333 Moscow, Russia
[2] Ioffe Institute,
194021 St. Petersburg, Russia

E-mail: f.solomkin@mail.ioffe.ru

*Received October 20, 2021*
*Revised October 25, 2021*
*Accepted October 25, 2021*

The phase composition, microstructure, and interphase interfaces of the disordered $CrSi_2-FeSi_2$ solid solution obtained by spontaneous crystallization (before and after annealing) have been investigated by scanning, transmission electron microscopy, electron diffraction, and X-ray energy dispersive spectrometry. The as-grown samples contained the phases of $CrSi_2$ with the $P6_422$ hexagonal structure and $FeSi_2$ with the $P4/mmm$ tetragonal structure. Annealing of the samples led to the phase transformation of tetragonal $FeSi_2$ into the orthorhombic modification $Cmca$. Precipitates of cubic iron monosilicide FeSi with space group $P213$, nano-precipitates of Si and silicon silicide $Cr_5Si_3$ with a tetragonal structure $I4/mcm$ were observed inside the $FeSi_2$ grains. Impurities of interstitial Cr atoms with a concentration up to 2.0 at% are found in iron (di)silicides grains in all samples. The structure of the $CrSi_2$ phase remains unchanged after annealing; the concentration of impurity iron atoms is about 0.7 at%. Orientation relationships between the crystal lattices of the phases are established and strains due to the mismatch of the crystal lattices are determined.

**Keywords:** chromium disilicide, iron disilicide, interphase interfaces, transmission electron microscopy, energy dispersive X-ray spectrometry.

DOI: 10.21883/SC.2022.02.53041.33

## 1. Introduction

Thermoelectrics based on 3*d* transition metal silicides are of interest for the production of thermoelectric generators and sensor devices due to their chemical and mechanical resistance in an oxidizing environment at high temperatures, their compatibility with silicon technology, and the possibility of choosing materials among them with *n*- and *p*-conductivity type. The particular interest in the creation of thermoelectric converters belongs to the synthesis of anisotropic multiphase materials. The phase interfaces are full third phase with own structure and properties and, depending on the ratio of the dimensional parameters of the microstructure, can play a decisive role in the physical properties.

The paper [1] show the principle possibility to create a mechanically strong material based on medium temperature thermoelectrics $CrSi_2$ and $FeSi_2$ with a high anisotropy of thermoelectric parameters. During directional crystallization the formation of a layered microstructure with periodic repetition of $CrSi_2$ and $FeSi_2$ layers was observed. $CrSi_2$ is non-toxic thermoelectric with *p*-type conductivity and forbidden band width of 0.35 eV has a significant power factor with a maximum of $45\,\mu W/(K^2 \cdot cm)$ at $T = 600$ K, it is able to work in aggressive environments without special protection. Textured $CrSi_2$ can be used to create anisotropic thermoelectric generators operating in a wide temperature range (200–1000 K) [2]. The material has a wide region of homogeneity, so the thermoelectric properties of the samples strongly depend on the synthesis conditions and stoichiometry [3].

Iron disilicide $FeSi_2$, like $CrSi_2$, is a non-toxic thermoelectric material capable of operating in aggressive environments without special protection. $FeSi_2$ forms crystals of two modifications: the high-temperature phase $\alpha$-$FeSi_2$ with a tetragonal structure and a metallic type of conductivity, and the low-temperature phase $\beta$-$FeSi_2$ with a rhombic structure — a semiconductor with a forbidden band width of 0.85 eV [4]. Annealing $\alpha$-$FeSi_2$ at a temperature corresponding to the solid-state phase transition (1070–1170 K) results in a polymorphic transformation into $\beta$-$FeSi_2$ phase. Staged annealing $\alpha$-$FeSi_2$ leads to a gradual transition from semimetal to semiconductor $\beta$-$FeSi_2$, without mechanical destruction of samples [5].

In the case of long-term directional crystallization (the Bridgman method) in the temperature zone corresponding to the solid-state phase transition, the initially crystallized high-temperature phase is annealed with its transformation into $\beta$-$FeSi_2$ [6]. It is known that during long-term directional crystallization due to different diffusion coefficients of the components of melt, which is in the temperature gradient, they are dispersed over the volume of the ingot. Therefore, in this work, spontaneous crystallization was used to identify the phase composition, defect states, and the state of phase interfaces after synthesis.

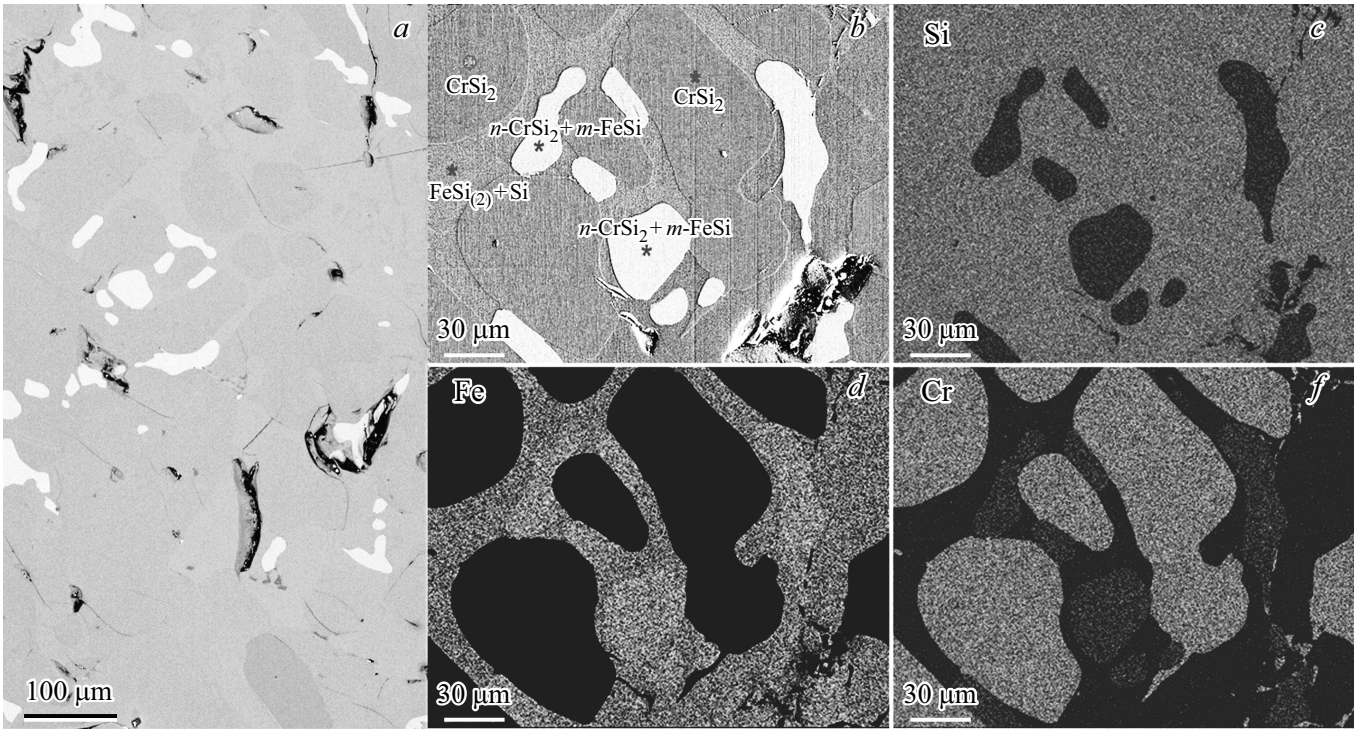


**Figure 1.** SEM-image (overview) of a disordered alloy $CrSi_2$ — $FeSi_x$ (*a*), phases distribution (*b*) and the corresponding distribution of the elements Si, Fe and Cr according to the EDS data (*c, d, f*).

## 2. Samples and study methods

The synthesis of samples was carried out in vacuum, by direct fusion of finely dispersed Cr, Fe and Si components, taken in a ratio corresponding to the $CrFeSi_4$ stoichiometry, at $T = 1723$ K. After spontaneous crystallization, the samples were annealed in air at $T = 1073$ K for 72 h.

Using scanning electron microscopy (SEM), transmission electron microscopy (TEM), electron diffraction (ED), and X-ray energy-dispersive spectrometry (EDS) the chemical and phase composition of samples before and after annealing in thin particles obtained by chipping of bulk samples was studied. SEM (FEI Scios with accelerating voltages in the range of 5–15 keV) was used to obtain survey images with the grains distribution of different phases. TEM, EDS and electron diffraction studies at the micro- and nanolevels were carried out in Tecnai Osiris microscope with accelerating voltage of 200 kV. The processing and interpretation of the data obtained were carried out using the Gatan Digital Micrograph (GATAN), JEMS [7], and ESPRIT (Bruker) programs. SEM-images and EDS provide the opportunity to estimate the size and shape of grains, the distribution of elements and phases in samples (Fig. 1).

## 3. Study results and discussion

The material of the annealed and unannealed samples consists of a mixture of randomly distributed grains of Cr and Fe silicide phases. The light grains in Fig. 1 correspond to phases with a higher average atomic number. For example, iron (di)silicide grains or combinations of iron silicide and chromium admixtures will always be lighter compared to grains of pure $CrSi_2$ (average atomic number 36) or combination of $FeSi_2$ and Si nanoprecipitations (average atomic number 32).

The analysis of TEM-images and electron diffraction patterns showed that $CrSi_2$ with the hexagonal structure $P6_422$ [8] is formed in the synthesized samples before their annealing and does not change its structure after annealing (Fig. 2). Quantitative EDS-analysis of unannealed samples showed that $CrSi_2$ grains can contain maximum 0.7 at% Fe, and $\alpha$-$FeSi_2$ up to 2 at% Cr. Tetragonal $\alpha$-$FeSi_2$ with $P4/mmm$ structure [9] after annealing transforms into $\beta$-$FeSi_2$ phase with rhombic structure $Cmca$ [10]. Besides, segregation of $Cr_5Si_3$ nanocrystals with a tetragonal lattice and elongated nanoprecipitates Si was observed inside grains $\beta$-$FeSi_2$, while grains $CrSi_2$ do not contain iron impurities or silicon precipitates. Thin layers of FeSi with cubic structure $P213$ [11] bordering to $CrSi_2$ were revealed. The Table lists the silicide phases in disordered $CrSi_2$–$FeSi_2$ alloys before and after annealing.

The analysis of the electron diffraction patterns made it possible to determine several orientation relationships for both types of alloy samples. It is common practice to express orientation relationships in terms of a plane and

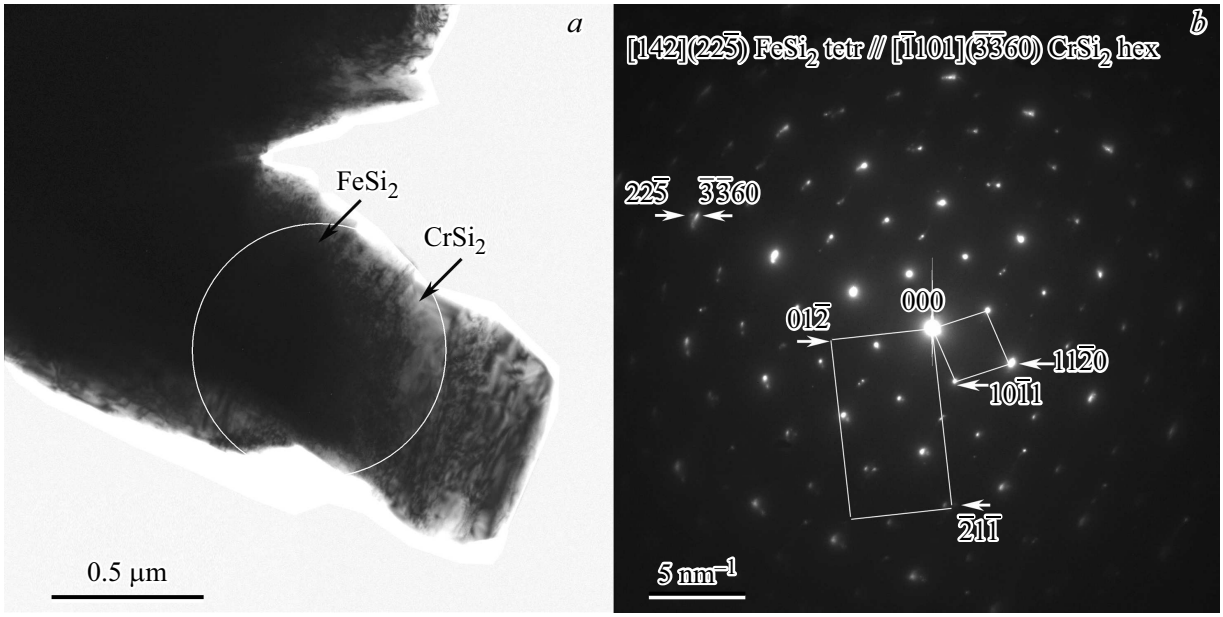


**Figure 2.** TEM-image ($a$) and electron diffraction pattern ($b$) with highlighted cells from $CrSi_2$ and $FeSi_2$ and orientation relations.

direction in one phase (precipitate) that are parallel to the plane and direction in another phase (matrix), for which the sample in an electron microscope is tilted to obtain a diffraction pattern in which the axes of the zone (the direction to the pattern plane) from both phases coincide. Orientation relations can be used to estimate mismatches between crystal lattices and possible deformations, as well as the degree of interface coherence.

Fig. 2 shows TEM-image of unannealed sample (Fig. 2, $a$) with the corresponding electron diffraction (Fig. 2, $b$), which contains reflections from hexagonal $CrSi_2$ and tetragonal $FeSi_2$. The following orientation relationships were revealed between the two phases in the experimental electron diffraction patterns:

- $[142](22\bar{5})$ $FeSi_2$ tetr // $[\bar{1}101]$ $(\bar{3}\bar{3}60)CrSi_2$ hex
- $[881](1\bar{1}0)$ $FeSi_2$ tetr // $[11\bar{2}0](2\bar{2}00)$ $CrSi_2$ hex

$\delta$ discrepancy between lattices, calculated by the formula

$$\delta = \frac{2(d_{Fe} - d_{Cr})}{d_{Fe} + d_{Cr}},$$

where $d_{Fe}$ and $d_{Cr}$ are interplanar distances, from the corresponding planes of two phases of Fe and Cr silicides ($d_{22\text{-}5}$ $FeSi_{2\,tetr} = 0.0696$ nm, $d_{3\text{-}360}$ $CrSi_{2\,hex} = 0.0738$ nm, $d_{1\text{-}10}$ $FeSi_{2\ tetr} = 0.1906$ nm, $d_{2\text{-}200}$ $CrSi_{2\ hex} = 0.1107$ nm) was $\sim 6\%$ for the first ratio and 0.5% — for the second.

For the annealed samples the following orientation relations and discrepancies $\delta \approx 1\%$ between the lattices $CrSi_2$ hex and $FeSi_2$ rhomb ($d_{6\text{-}33\text{-}3}$ $CrSi_{2\ hex} = 0.0697$, $d_{0\text{-}88}$ $FeSi_{2\ rhomb} = 0.0691$ nm):

- $[1\,13\,\bar{1}4\,3](6\bar{3}3\bar{3})$ $CrSi_2$ hex // $[311]$ $(0\bar{8}\bar{8})FeSi_2$ rhomb.

As mentioned above, in the samples after annealing the precipitates of cubic iron monosilicide FeSi were observed in grains of hexagonal $CrSi_2$ in the form of thin

Phase composition of disordered alloy $CrSi_2-FeSi_2$ before and after annealing

| Phases | Before annealing | | After annealing | |
|---|---|---|---|---|
| | Phase | Spatial group | Phase | Spatial group |
| Fe silicide | $FeSi_2$ tetr | $P4/mmm$ | $FeSi_2$ rhomb<br>FeSi cube | $Cmca$<br>$P213$ |
| Cr silicide | $CrSi_2$ hex | $P6_422$ | $CrSi_2$ hex<br>$Cr_5Si_3$ tetr | $P6_422$<br>$I4/mcm$ |
| Silicon | Not revealed | | Si cube | $Fd-3m$ |

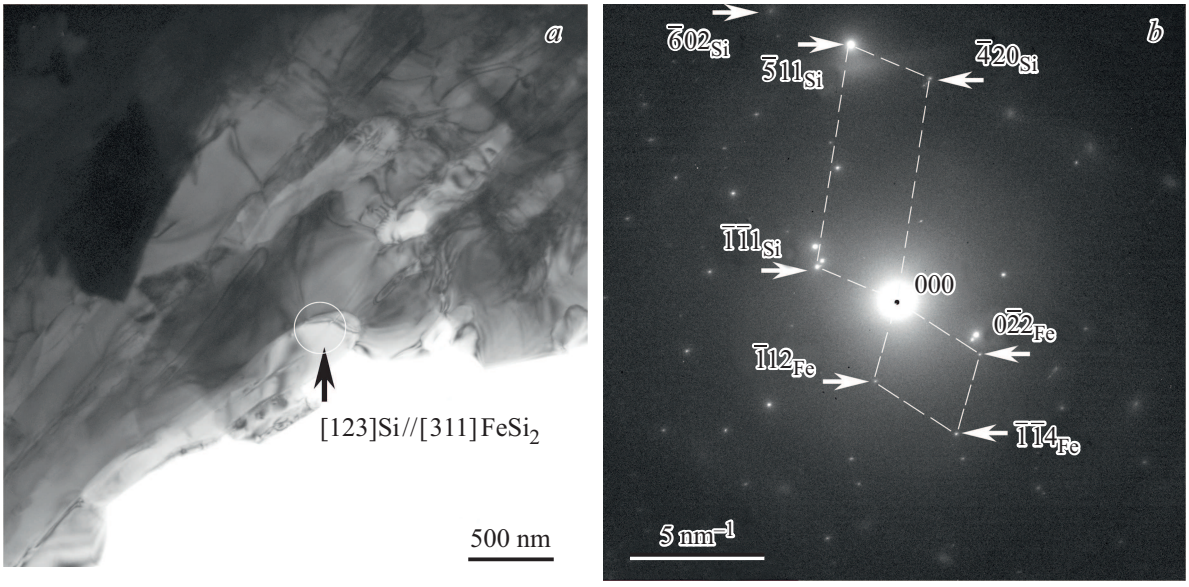


**Figure 3.** TEM-image of grain $\beta$-$FeSi_2$ with Si nanoprecipitations ($a$), electron diffraction pattern ($b$) with reflections from $\beta$-$FeSi_2$ and Si obtained from the circled area on the TEM- image.

rods with a width of $\sim 50$ nm. Nanoprecipitates of the tetragonal phase $Cr_5Si_3$ [12] and cubic Si [13] (Fig. 3) were detected in matrix grains of rhombic $FeSi_2$. The orientation relationships between the matrix grains $CrSi_2$ and $FeSi_2$ and nanoprecipitations of secondary phases after annealing are presented below:

- $[12\bar{3}0](0003)$ $CrSi_2$ hex // $[120](\bar{2}10)$FeSi cube, $\delta \approx 8\%$.
- $[112](\bar{1}\bar{5}3)$ $FeSi_2$ rhomb // $[379](223)Cr_5Si_3$ tetr, $\delta \approx 0.4\%$.
- $[311](\bar{2}\bar{2}8)$ $FeSi_2$ rhomb // $[123](60\bar{2})$Si cube, $\delta \approx 8\%$.

To determine the mismatch between the crystal lattices of the phases the following interplanar distances were taken: $d_{0003}$ $CrSi_{2\,\mathrm{hex}} = 0.2123$ nm, $d_{\text{-}210}$ $FeSi_{\mathrm{cube}} = 0.2035$ nm, $d_{\text{-}1\text{-}53}$ $FeSi_{2\,\mathrm{rhomb}} = 0.1326$ nm, $d_{233}$ $Cr_5Si_{3\,\mathrm{tetr}} = 0.1321$ nm, $d_{\text{-}2\text{-}28}$ $FeSi_{2\,\mathrm{rhombus}} = 0.0933$, $d_{60\text{-}2}$ $Si_{\mathrm{cube}} = 0.0862$ nm. Thus, all experimentally observed orientational relations indicate the formation of semi-coherent interfaces, with stress relaxation occurring with the help of misfit dislocations. Obviously, other orientational relations in different directions with other numerical mismatches are also possible.

The deformations of the parameters mismatch of the lattices of different phases in materials, as well as the mismatch of their thermal expansion coefficients generate mechanical stresses, which are removed by the formation of defects, for example, cracks and cavities, which are revealed on the polished surface of both annealed and unannealed samples (Fig. 1, $a$). The deformation caused by differences during thermal expansion can be represented as

$$\delta_{\mathrm{therm}} = \frac{d_1^{RT}(\alpha_1 - \alpha_2)\Delta T}{d_2^{RT}(1 + \alpha_2 \Delta T)},$$

where $d_1^{RT}$ and $d_2^{RT}$ are the corresponding interplanar distances in lattices of two phases at room temperature, $\Delta T$ is difference between synthesis temperature and room temperature, $\alpha_1$ and $\alpha_2$ are coefficients of thermal expansion of phases of two neighboring grains.

The values of the coefficients of linear thermal expansion (averaged considering anisotropy) for $\beta$-$FeSi_2$ are in the range $10.6-11.8 \cdot 10^{-6}\,\mathrm{K}^{-1}$ [14], and for $CrSi_2$ the range is $10.6-14.2 \cdot 10^{-6}\,\mathrm{K}^{-1}$ [15] at temperatures from room temperature to 1173 K. The contribution to the appearance of lattice deformations of the solid solution due to the difference in thermal expansion coefficients is $\sim 0.5\%$, while the mismatch between the lattice parameters of $FeSi_2$ and $CrSi_2$ in unannealed samples reaches 6%, which is the main cause of stresses, during the relaxation of which defects are formed. After the solid solution annealing several more phases are precipitated with 8-percent mismatch between the lattices of matrix grains and precipitates, which can also lead to stresses and, ultimately, to the appearance of cracks in the samples.

## 4. Conclusion

1. The data obtained in the study of the microstructure and composition of disordered alloy with $CrFeSi_4$ stoichiometry initially incorporated during synthesis indicate the stability of $CrSi_2$ phase, which after annealing does not contain neither iron impurities nor silicon precipitates.

2. Tetragonal $\alpha$-$FeSi_2$ after annealing turns into $\beta$-$FeSi_2$ phase with rhombic structure in which the presence of $Cr_5Si_3$ silicide nanoprecipitates with a tetragonal lattice and elongated Si precipitates is observed, which, in the case of directed crystallization of the alloy, can be a

technological factor to control the physical properties of the composite.

3. Numerical orientational mismatches were established between the crystal lattices of the phases in different crystallographic directions. Relaxation of deformations caused by mismatches between lattices can lead to the formation of dislocations at interfaces with subsequent cracking of the material.

### Funding

The work was supported by the Ministry of Science and Higher Education of the Russian Federation.

### Conflict of interest

The authors declare that they have no conflict of interest.

## References

[1] F.Yu. Solomkin, V.K. Zaitsev, S.V. Novikov, A.Yu. Samunin, D.A. Pshenai-Severin, G.N. Isachenko. ZhTF, **84**, 106 (2014) (in Russian).
[2] M.I. Fedorov, V.K. Zaitsev. *Handbook of Thermoelectric*, ed. by D.M. Rowe (N.Y., CRC press., 2006) p. 31-2.
[3] F.Yu. Solomkin, V.K. Zaitsev, S.V. Novikov, Yu.A. Samunin, G.N. Isachenko. ZhTF, **83** (2), 141 (2013) (in Russian).
[4] U. Birkholz, E. Gross, U. Stohrer. *Handbook of Thermoelectrics*, ed. by D.M. Rowe (N.Y., CRC Press, 1995) p. 287.
[5] F.Yu. Solomkin, D.A. Pshenai-Severin, A.Yu. Samunin, G.N. Isachenko. *Tez. dokl. Mezhgos. konf. „Termoelektriki i ikh primeneniya — 2014“* (SPb., Rossiya, 2014) s. 407. (in Russian)
[6] F.Yu. Solomkin, A.Yu. Samunin, N.F. Kartenko, A.S. Kolosova. *IX Mezhgos. sem. „Termoelektriki i ikh primeneniya — 2004“* (SPb., Rossiya, 2004) s. 260. (in Russian)
[7] P. Stadelmann. 2017. JEMS, program description can be found in https://www.jems-swiss.ch/
[8] K.Tanaka, K. Nawata, M. Koiwa, M. Yamaguchi, H. Inui. Mater. Res. Soc. Symp. Proc., **646**, N 4.3.1 (2001).
[9] B. Aronsson. Acta Chem. Scand., **14**, 1414 (1960).
[10] Y. Dusausoy, J. Protas. Acta Cryst. B, **27**, 1209 (1971).
[11] L. Vocadlo, K.S. Knight, G.D. Price, I.G. Wood. Phys. Chem. Miner., **29**, 132 (2002).
[12] C.H. Dauben, D.H. Templeton, C.E. Myers. J. Phys. Chem., **60**, 443 (1956).
[13] W.L. Bond, W. Kaiser. J. Phys. Chem. Sol., **16**, 44 (1960).
[14] M. Imai, Y. Isoda, H. Udono. Intermetallics, **67**, 75 (2015).
[15] B.S. Rabinovich, I.Z. Radovsky, P.V. Gel'd. Poroshkovaya metallurgiya, **7**, 879 (1968). (in Russian).

**Publication of conference materials completed.**